Magma migration, folding, and disaggregation of migmatites in the Karakoram Shear Zone, Ladakh, NW India

Roberto F. Weinberg[†]
Geordie Mark*
School of Geosciences, Monash University, Clayton, Vic 3800, Australia

ABSTRACT

Efficient extraction of granitic magma from crustal sources requires the development of an extensive permeable network of melt-bearing channels during deformation. We investigate rocks that have undergone deformation and melting within the Karakoram Shear Zone of Ladakh, NW India, in which leucosome distribution is inferred to record the permeable network for magma extraction. Delicate structures preserved in these rocks record the development of this permeable magma network and its subsequent destruction to form a mobile mass of melt and solids, resulting from the interplay between folding and magma migration. During folding, magma migrated from rock pores into layer-parallel and axial-planar sheets, forming a stromatic migmatite or metatexite with two communicating sets of sheets, intersecting parallel to the fold axis. Once the network was developed, folding and stretching was eased by magma migration and slip along axial planar magma sheets. Folding and magma migration led to layer disaggregation, transposition, and the formation of a diatexite where rock coherency and banding were destroyed. A number of structures developed during this process such as cuspate fold hinges, disharmonic folds, truncated layering, shear along axial planar leucosomes, and flow drag and disruption of melanosomes. In this system, magma migration was an integral part of deformation and assisted the folding and stretching of metatexites, while folding gave rise to a magma sheet network, now preserved as leucosomes, as well as the pressure gradients that drove magma migration and the breakup of the metatexite. Thus, metatexite folding increased melt interconnectivity, while magma mobility increased strain rate and released differential stresses.

Keywords: diatexite, metatexite, migmatite, folding, transposition, granites.

INTRODUCTION

Mechanisms that allow draining of granitic magma from regions of crustal anatexis and that lead to large magma accumulations, such as plutons and batholiths, control not only the evolution of granitic systems but also crustal differentiation and crustal rheological and thermal evolution (Hollister and Crawford, 1986). How magma is transferred from source to sink is currently the most controversial aspect of granitic systems. It is the nature of the magma network in the source that ultimately controls transfer through cold, subsolidus crust (Weinberg, 1999). Dikes are potentially an effective means of transferring magmas between source and pluton, however, dikes will only be efficient if the source is capable of providing high magma fluxes into the dike so as to inhibit magma from freezing in transit. This paper reports on the evolution of a remnant magma network, now preserved as leucosomes in a migmatite within the transpressive Karakoram Shear Zone, in the Tangtse gorge, Pangong Range, Ladakh, NW India (Fig. 1). This gorge exposes rocks that have undergone synkinematic melting at upper amphibolite facies in the presence of a water-rich volatile phase and have acted simultaneously as a transfer zone of deeper magmas, recorded by the intrusion of leucogranite sheets hundreds of meters wide (Fig. 2). These Miocene leucogranites in leucosomes and in sheets are broadly of the same age and modal composition as those forming the Karakoram Batholith (Searle et al., 1998; Weinberg et al., 2000; Weinberg and Searle, 1998), exposed northeast of the gorge (Fig. 1), and thus the crustal section exposed in the gorge is interpreted to represent a magma transfer and production zone to the batholith. This region is similar to the transpressive shear zones through anatectic rocks of the Armorican terrane in Brittany (Brown, 1978; Brown and D'Lemos, 1991) and its counterpart in the Iberian Peninsula (Hutton and Reavy, 1992).

Leucosomes are material crystallized from melt-rich bands developed by melt segregation from the solid matrix during anatexis. Leucosomes preserved in exposed anatectic migmatites do not generally represent pure melts but are the result of accumulation of residual and newly grown magmatic crystals, left behind by melt which escaped the system (Marchildon and Brown, 2003). The geometry of leucosome networks in migmatites is thus only a partial record of the network that existed at the time of melt migration. They are nevertheless the best record available. Leucosomes are interlayered with melt-poor bands, known as melanosomes, which generated and lost significant volumes of melt and are composed either of residual or peritectic minerals, or known as mesosomes, which generated a lower melt volume. Interlayering of leucosomes, mesosomes, and melanosomes forms banded rocks. Where banding is well preserved, indicating that the rock did not lose coherency during melting, the migmatite is referred to as metatexite, or as stromatic migmatite. Because metatexites maintain a solid framework, melt can be extracted from their solid matrix (Brown, 1973). As the melt fraction increases, either through further melting (White et al., 2005) or through melt injection, the solid matrix loses cohesion with wholesale disruption of preexisting structures, giving rise to a diatexite migmatite (Brown, 1973). The transition from metatexite to diatexite therefore corresponds to significant rock weakening related to the loss of the solid skeleton (Burg and Vanderhaeghe, 1993), with major implications for crustal straining.

The melt fraction required to disrupt the solid matrix depends on crystal size and shape distribution, their preferred orientation, and the nature and intensity of straining (Miller et al.,

[†]E-mail: roberto.weinberg@sci.monash.edu.au
*Present address: Haywood Securities Inc., 2000, 400 Burrard St., Vancouver, British Columbia V6C 3A6, Canada

GSA Bulletin; July/August 2008; v. 120; no. 7/8; p. 994–1009; doi: 10.1130/B26227.1; 15 figures.

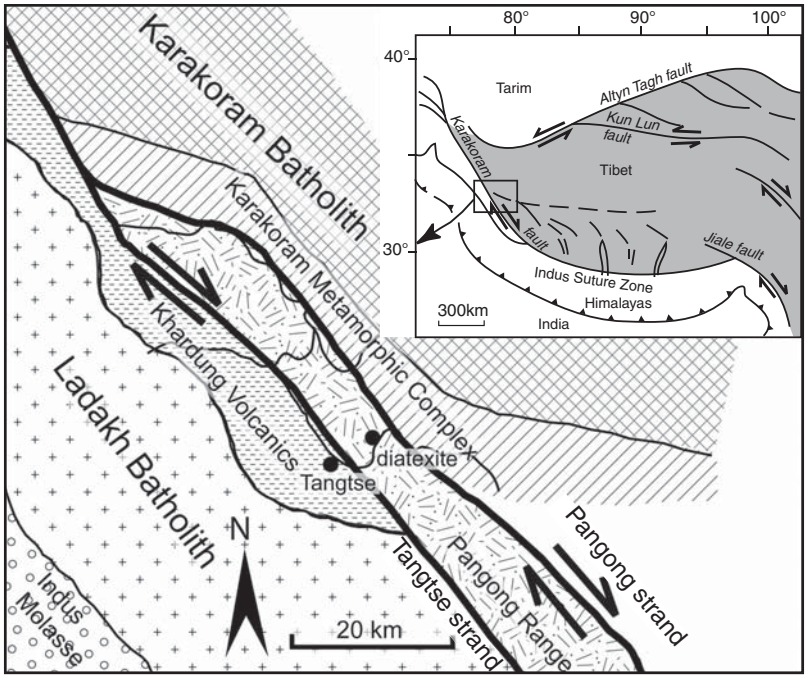

Figure 1. Geological map of the Karakoram Shear Zone in NW Ladakh, India. The Ladakh Batholith and Khardung Volcanics represent an early, pre-collisional calc-alkaline sequence. The diatexite layer studied in this paper is exposed in the gorge transecting the Pangong Metamorphic Complex which underlies the Pangong Range, which is bound on either side by the Pangong and the Tangtse strands of the Shear Zone. The Karakoram Metamorphic Complex crops out to the NE and the Karakoram Batholith crops out to the SW of the Pangong Range.

1988; Rosenberg and Handy, 2005; van der Molen and Paterson, 1979; Vigneresse et al., 1996). It follows that melt redistribution within metatexites, without an increase in overall melt fraction, can cause its disruption (Sawyer, 1998). Tectonically driven deformation plays a crucial role in enhancing melt segregation from rock pores from grain to outcrop scale, and in redistributing melt within the rock mass (Brown and Solar, 1998; McLellan, 1988; Sawyer, 1991). Thus, crustal deformation, melt segregation, and redistribution are all intimately related to the breakdown of the solid framework of metatexites (Sawyer et al., 1999).

A number of papers have investigated the geometries of granitic magma segregation through the study of structural relationships between leucosomes and their surroundings (Brown, 1994, 2005; Brown and Solar, 1998; Collins and Sawyer, 1996; D'Lemos et al., 1992; Hand and Dirks, 1992; Sawyer et al., 1999; Vernon and Paterson, 2001). Few have studied the path taken by magma moving along anatectic zones (Allibone and Norris, 1992; Greenfield et al., 1998; Hand and Dirks, 1992; Sawyer, 1998, 1999) possibly as a result of the morphologic complexity of leucosomes, as pointed out by Sawyer (1999), and possibly as a result of the absence of unambiguous indicators of the direction of magma migration. The purpose of this paper is to examine the evolution of the geometry of magma migration paths during fold transposition within the Karakoram Shear Zone, and to determine how folding and melting interacted to destroy preexisting layering and disaggregate the rock mass to form a tectonic diatexite.

REGIONAL GEOLOGY

The rocks exposed in the Tangtse gorge are part of the Pangong Metamorphic Complex (Fig. 2). This complex was exhumed within an ~7-km-wide pop-up structure (Dunlap et al., 1998; Weinberg et al., 2000), part of the 1000-km-long, dextral Karakoram Shear Zone, one of the greatest strike-slip faults that accommodate the lateral extrusion of Tibet in response to the northward indentation by India (Brown et al., 2002; Molnar and Tapponnier, 1975, 1978; Searle et al., 1998; Valli et al., 2007; Weinberg et al., 2000). The metasedimentary sequence exposed (Fig. 2) is characterized by a biotite-rich sequence of metamorphosed psammites, semipelites, and pelites (Bt psammite in Fig. 2) thick sequences of calc-silicate, and a sequence of hornblende-bearing rocks, assumed to represent a volcanic or volcaniclastic sequence (Hbl-bearing sequence in Fig. 2), interlayered with narrow and now disrupted bands of calc-silicates. A calc-alkaline granitic suite intruded the metasedimentary sequence, forming two biotite-hornblende granodiorite bodies with minor diorite and granite bands, in the gorge section. The biotite-rich clastic sequence, the hornblende-bearing volcaniclastic sequence, and the calc-alkaline granodiorite intruding them have undergone partial melting, forming migmatites that feed leucogranite dikes and irregular pods of widths up to hundreds of meters to a kilometer (Weinberg, 1999; Weinberg and Searle, 1998).

The biotite-rich clastic sequence in the gorge is typically composed of biotite, plagioclase, and quartz and minor fine-grained garnet and tourmaline. The hornblende-bearing sequence is typically composed of hornblende, biotite, plagioclase, and quartz, and varying modal proportions give rise to gradation between biotite, hornblende gneisses and amphibolites. Rolland and Pêcher (2001) estimated upper amphibolite conditions for rocks in this area with T ~700–750 °C and P ~4–5 kbar. During metamorphism, the biotite-rich clastic sequence is interpreted to have melted in situ without the production of obvious peritectic minerals. Garnet is thought to pre-date melting (rather than being a peritectic phase) because: (a) K-feldspar, which is generally a product of garnet-producing dehydration melting involving biotite, is absent (Spear, 1993); and (b) garnet distribution is generally unrelated to the distribution of either leucosomes or refractory melanosomes.

The hornblende-bearing sequence, in contrast, is interpreted to have undergone melting accompanied by the growth of peritectic, euhedral porphyroblasts of poikilitic hornblende. Typical leucosomes related to the melting of the biotite-rich clastic sequence vary from granodiorite to granite, and are composed of quartz-plagioclase-K-feldspar-biotite-muscovite-tourmaline-garnet. Melting is inferred to have occurred at the wet granite solidus, involving H_2O as a free phase, and we refer to this process as wet melting. The presence of water during metamorphism would also explain the growth of peritectic hornblende in the hornblende gneisses (Berger et al., 2007; Mogk, 1992).

Water infiltrated into this region from an unknown source. The most obvious water source is the subsolidus rock packages exposed to the NE and SW of the Pangong Range, which were underthrust by the pop-up structure that exhumed the Pangong Metamorphic Complex. During partial melting, some biotite may have been dissolved by the melts or may have been

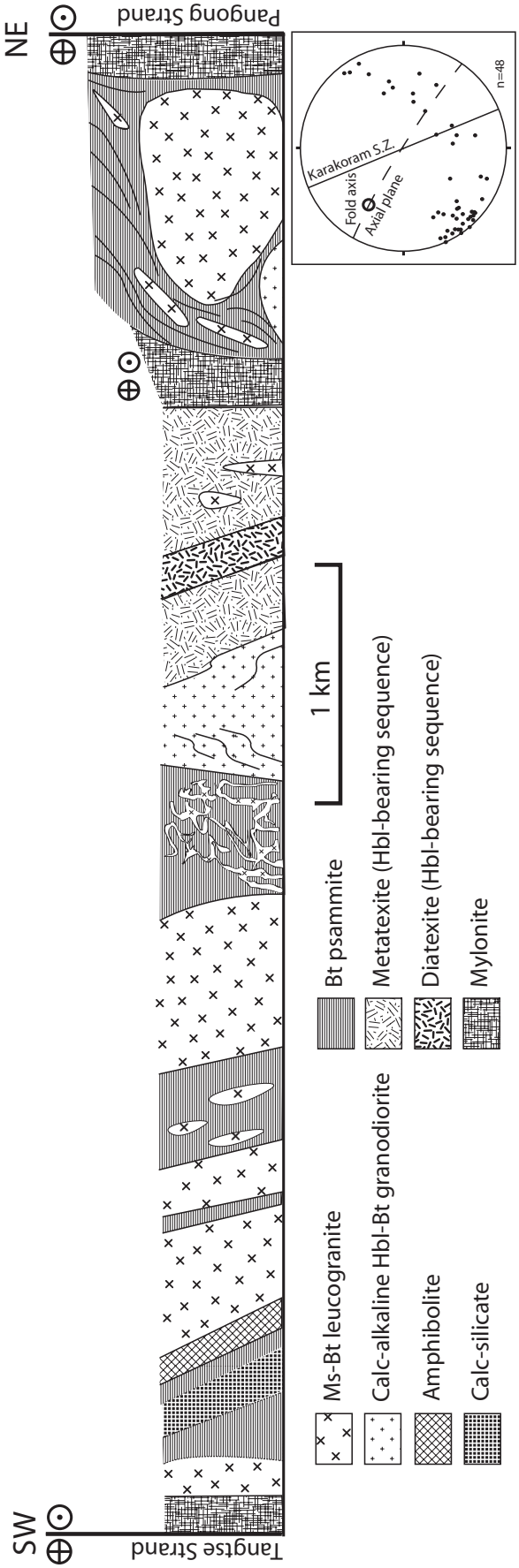

Figure 2. Geological cross section of the Pangong Metamorphic Complex exposed in the gorge indicating the position of the diatexite layer. Insert: stereonet defining NW-trending upright folds within this cross section of the Karakoram Shear Zone.

involved in melting reactions leading to the production of peritectic hornblende in the presence of a water-rich volatile phase (Lappin and Hollister, 1980; Mogk, 1992). Most of the biotite, however, remained stable and was dragged and disaggregated by melt migration as solids (Milord et al., 2001) together with preexisting and newly grown peritectic hornblende (Fig. 3).

SHRIMP U-Pb zircon dating yielded a crystallization age between 18 and 13.5 Ma for leucogranite samples from the gorge (Phillips et al., 2004; Searle et al., 1998). Interestingly, two of the dated leucogranites contained inherited zircons dated ca. 63 Ma and ca. 106 Ma (Searle et al., 1998). These ages are similar to those obtained for the calc-alkaline Ladakh Batholith (Honegger et al., 1982; Weinberg and Dunlap, 2000), which crops out immediately south of the Karakoram Shear Zone (Fig. 1). Although crystallization ages of the calc-alkaline suite in the gorge are currently unavailable, Rb-Sr whole rock geochronology yielded and age of 118 ± 18 Ma (Ravikant, 2006). It is therefore inferred that anatexis of this suite may have contributed with melt and the older zircons to form the leucogranite sheets. Ar-Ar data derived from the leucogranites indicate rapid cooling during the period between 17 and 13 Ma, at which time the Ladakh Batholith to the SW had already cooled to below <150 °C (Dunlap et al., 1998). North of the Karakoram Shear Zone, lower grade biotite-staurolite-garnet schists, calc-schists, marbles, and amphibolites (Dunlap et al., 1998) form the Karakoram Metamorphic Complex.

The Karakoram Shear Zone is characterized by oblique slip with components of dextral strike slip and reverse slip (Weinberg et al., 2000). In the Tangtse gorge, the Karakoram Shear Zone trends toward 140° and dips subvertically, generally containing a stretching lineation plunging toward 30–40° NW (Weinberg et al., 2000), but ranging between those values and 0° to 10° SE. High-strain, mylonitic zones are concentrated in two main shear zones, one on either margin of the 7-km-wide zone: the Pangong strand bounds the Pangong Range to the NE, and the Tangtse strand bounds it to the SW (Dunlap et al., 1998).

Between these two strands, rocks are also sheared but generally not as intensely. In less strained areas, rocks preserve folds with steep axial planar foliation trending between 120° and 140° and plunging moderately NW (Fig. 2 insert). These folds are interpreted to have formed contemporaneously with shearing, because they are kinematically compatible, and because shearing and folding were both contemporaneous with anatexis. All rocks, including leucogranite sheets and leucosomes, are overprinted by either shear planes or axial planar foliation. Typically, though, leucosomes or leucogranites cropping

out within the gorge, away from the bounding shear zones, are characterized by relatively low strain indicated by mineral preferred orientation, bent plagioclase lamellar twins, myrmekite, and undulose extinction plus subgrains in quartz. Thus, the contemporaneity of events suggests that the shear zone underwent anatexis during transpressive deformation, driven by ~N-S directed shortening (Weinberg et al., 2000).

RESULTS

The focus of this paper is a diatexite layer ~300 m wide trending NW-SE and dipping steeply. This diatexite developed within the hornblende-bearing sequence and is sandwiched between metatexites composed of hornblende-bearing leucosomes and hornblende-bearing gneisses and amphibolites (Fig. 2). In the diatexite, there is a variety of leucosome types of different modal compositions and textures. They vary from pegmatitic to medium-grained, and from leucogranites to leucotonalites, and contain different proportions of biotite and hornblende. Some leucosomes have minor muscovite, tourmaline, titanite, and garnet.

The diatexite includes metric to decametric regions where folded metatexites are preserved and which record the stepwise breakup of layer continuity. Rocks preserved in this region are similar to the intermediate hornblende gneisses and amphibolites found in surrounding metatexites. Descriptions of the stepwise breakup of metatexites are based on either the predominantly steep outcrop exposures, or on large (1–80 m^3) displaced but locally derived angular blocks in the steep scree immediately below the outcrops. Blocks are particularly useful because they allow 3D investigation. All photographs presented are taken at high angle to the axial planar foliation and approximately down fold plunges, unless stated otherwise. Many of the features described may be found in a number of figures; however, in the text, we refer only to the clearest examples.

The most significant feature linking metatexites and diatexites is that the axial planar foliation of folds in metatexites is parallel to the irregular banding in diatexites, defined by partly disaggregated layers and mafic schlieren (Fig. 3). Figure 4 summarizes a number of features of folds in the preserved metatexites. Folds are commonly disharmonic, varying in wavelength and amplitude over short distances (Fig. 4B). Folds have layer-parallel leucosomes linked continuously with leucosomes parallel to the axial planar orientation, which cut through fold hinges and truncate layers (Figs. 5A–5C).

Fold hinges are commonly cuspate (Figs. 4 and 6) with or without axial planar leucosomes (Figs. 5A and 6). Figure 6A shows the relationship between a cuspate fold hinge and the breakup of a competent amphibolite layer. The displacement and partial disruption of the amphibolite block along the hinge zone, the abrupt and intense dragging of layers into the cuspate fold hinge, and layer truncation along the hinge zone all suggest mass flow and magma loss from left to right along the hinge zone. Also, pegmatitic material accumulated on the left-hand side of the amphibolite layer, further suggesting that migration direction (and possibly way-up, Burg and Vanderhaeghe, 1993) was to the right. Mass loss along cuspate hinges is also inferred for Figure 6B, where melanosome bands merge along the cuspate, stretched hinge zone as a result of the loss of intervening leucosome bands. Cuspate hinges and truncated layers may also exist in the absence of axial planar leucosomes (Fig. 6C). A feature of these folds is that layer width changes abruptly or layers completely disappear across truncating axial planar foliation (Fig. 6C).

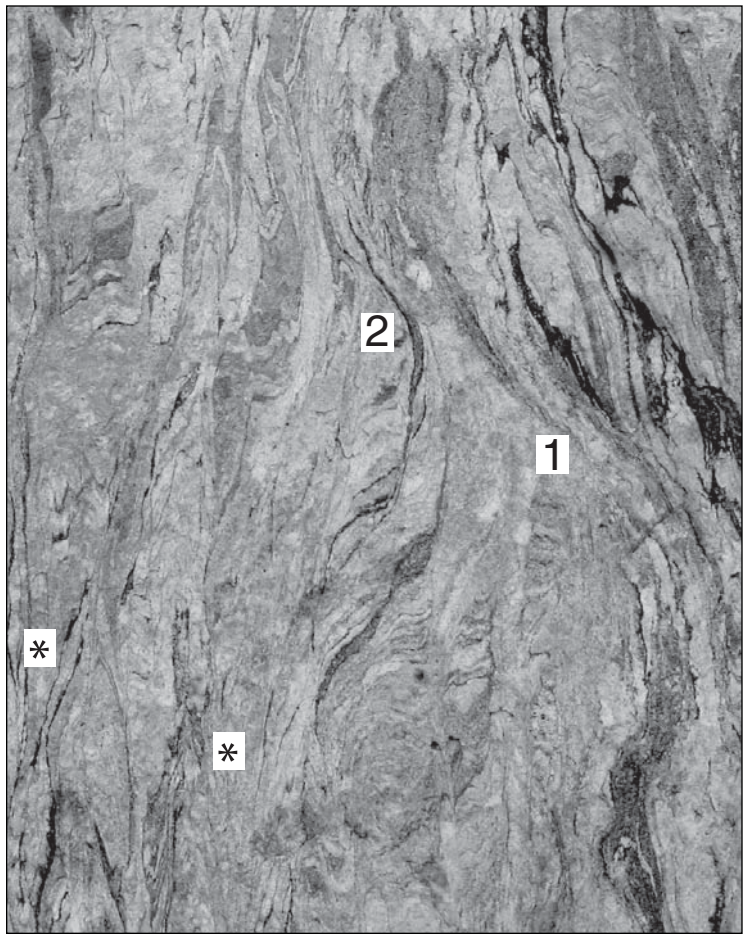

Figure 3. Vertical outcrop of hornblende-bearing sequence within the diatexite zone in Figure 2, showing advanced stages of transposition where folds are tight (*) and limbs nearly transposed (1). Layers in metatexite defining asymmetric folds are dragged upward into a transposed zone (2). Note antiformal fold closures (*) and absence of synformal closures. Scale: vertical side of image is 1.5 m.

In Figure 7, a cauliflower-shaped pegmatite (Burg and Vanderhaeghe, 1993) is in the concave side of an open fold. The pegmatite has irregular and undefined boundaries with the migmatite and intrudes the amphibolite as irregular dikelets with sharp contacts. These differences, added to the amplification of the fold defined by ghost stratigraphy in the pegmatite, suggest that pegmatitic magma segregated from the migmatite into the hinge zone, where it ponded and intruded the impermeable amphibolite. In Figure 8, leucosomes cut across a melanocratic layer, dragging and disaggregating mafic layers, which form cuspate schlieren. These become increasingly diffuse to the right, suggesting magma flow in that direction. In Figure 9, another typical feature of hinge zones is shown, where a decrease in wavelength of

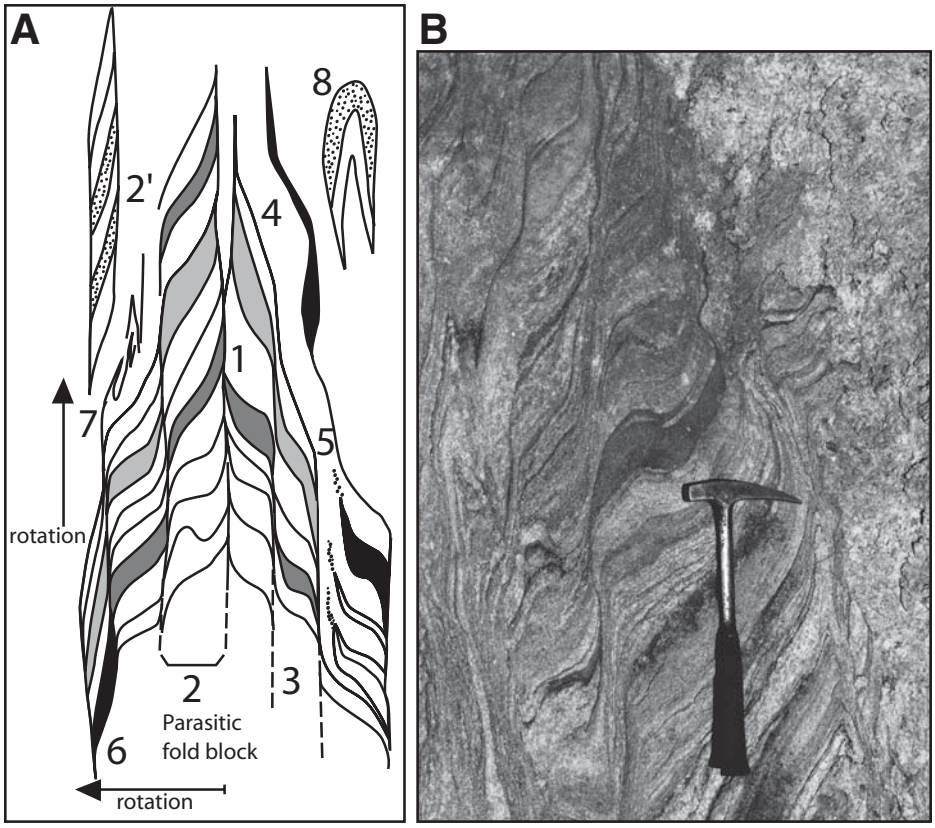

Figure 4. (A) Schematic fold profile summarizing the main features of magma-assisted fold transposition in Tangtse. Lenses with different tones of gray and in black represent schematically melanosomes and mesosomes. (1) Layer truncation across cuspate hinge zone, with or without axial planar leucosome. Cusps point outward from the fold core. (2) Limbs are defined by asymmetric "parasitic fold blocks" bound by well-developed, axial-planar foliations. Inside each parasitic fold block, folds are disharmonic with varying profiles and degrees of rotation toward the axial planar orientation. Parasitic fold blocks can be found in fully transposed parts of the diatexite as remnants of the transposition process (2′). (3) Axial planar foliation acted as shear planes accommodating considerable fold stretching. Such foliations may be filled with mafic residual material (melanosome), leucocratic material (leucosome), or mesocratic material. Layers may be continuous across axial planar foliation (left of 3 in figure), or may be truncated and discontinuous (right of 3). (4) Leucogranite dike trends diagonally across the fold from outer parts of limbs toward the fold closure in a manner broadly conformable with the shape of the fold. This is achieved by axial planar leucosomes side-stepping inward through layer-parallel leucosomes. (5) Mafic minerals are dragged from melanocratic layers into the axial planar leucosomes and dikes forming schlieren. (6) Parasitic fold blocks undergo increasing rotation toward the transposition plane, outward from the hinge zone (arrow labeled with "rotation"). (7) Fully transposed regions are characterized by schlieric diatexites containing remnant structures of the transposition process, such as an individual asymmetric fold block (2′), and rootless folds (8). (B) Example of parasitic fold block rotation, and axial planar leucosomes on fold limb.

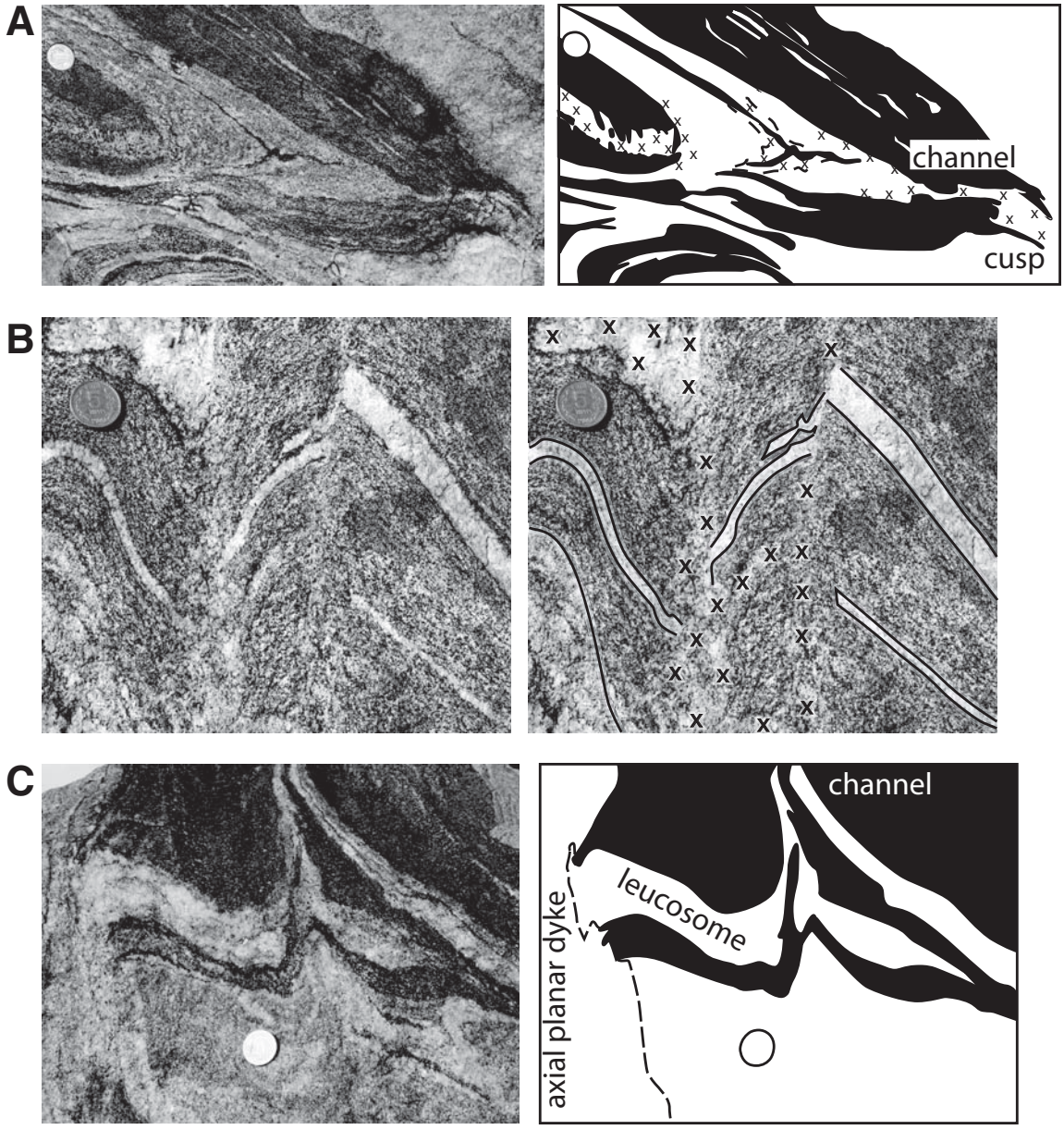

Figure 5. Some typical features associated with metatexite folds. (A) Leucosome in fold hinge zone, cutting across mafic layers forming a cuspate hinge on the right, defined by dragged and reoriented biotite and hornblende grains. Leucosomes are diffuse in the gneissic layer and more focused in mafic layers. Melt is interpreted to have moved to the right, from the fold core on the left, outward, forming a melt channel through the less permeable mafic layer which has disaggregated the cuspate fold tip. (B) Irregular axial-planar leucosomes with poorly defined margins in fold hinge zones (marked with x in line drawing) merging continuously with layer-parallel leucosomes with sharp margins and narrow (mm-wide) melanosome rims. Axial-planar leucosomes are interpreted to represent melt extraction paths that have partly drained layer-parallel leucosomes causing disruption and truncation. (C) Metatexite truncated on the left-hand side by a gray axial planar dike with diffuse internal banding parallel to its margin. Leucosome and melanosome layers fold into a narrow channel through a biotite amphibolite layer. Melanosome layer is incipiently disrupted by the process. All images from blocks.

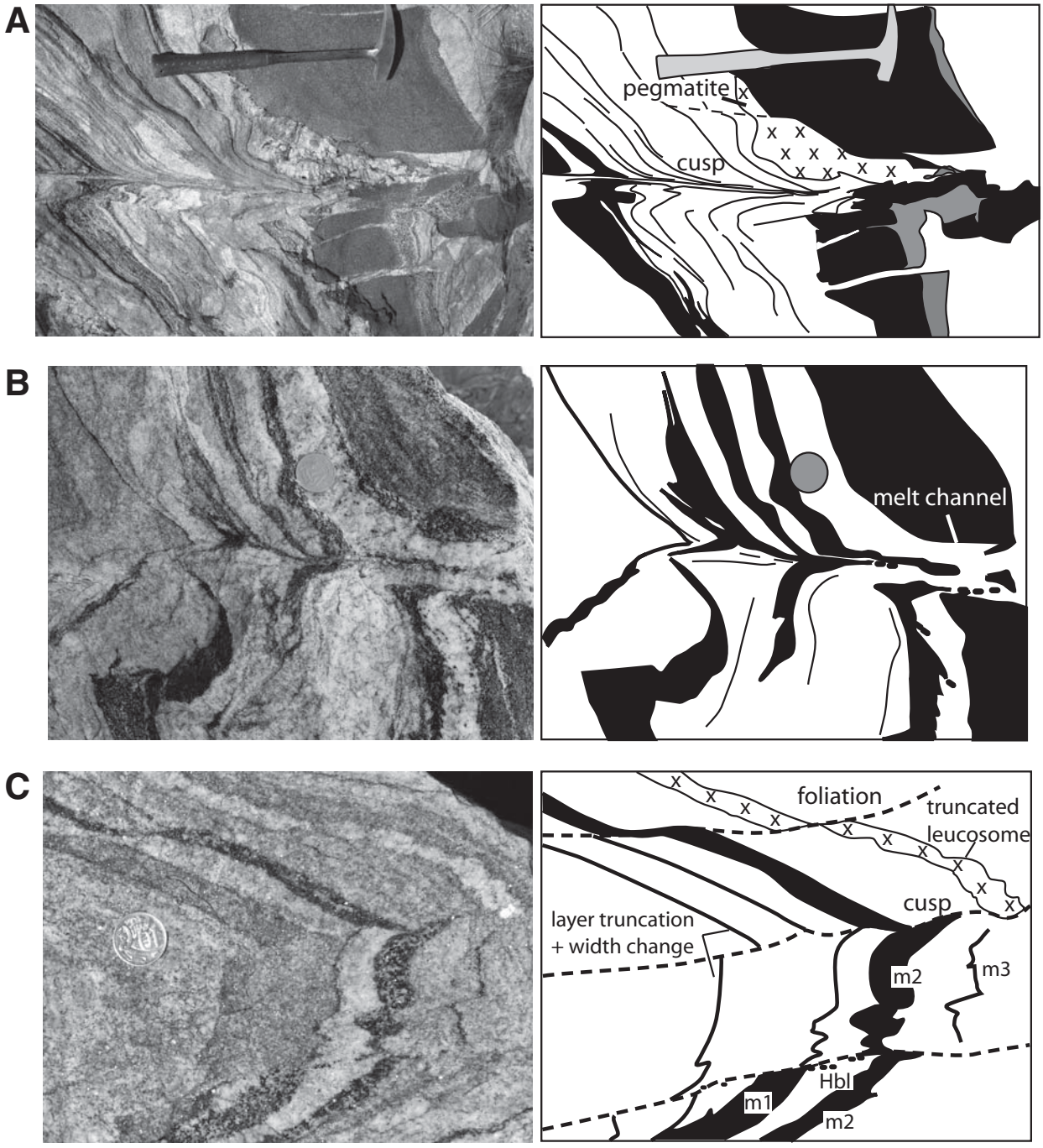

Figure 6. Cuspate hinge zones: (A) A tight, cuspate hinge zone is linked to a pegmatite body (close to hammer) in contact with broken and rotated parts of a competent amphibolite layer. The cuspate fold hinge, the pegmatite, and the breakup of the amphibolite layer suggest that melt once drained through the hinge zone (see Fig. 5A) and that the fold cusps point toward the direction of melt flow. Pegmatite accumulation on one side of the amphibolite suggests ponding before amphibolite disaggregation. (B) Dragging of melanosomes and leucosomes toward a fold hinge that cuts across a competent amphibolite layer on the right-hand side, interpreted to be a melt channel. Melanosome bands merge into the cuspate hinge zone indicating loss of leucosome material. Note melanosomes are not continuous layers, but thin out laterally. (C) Fold with cuspate hinge zone and well-developed, leucosome-free axial planar foliation. Layers are abruptly truncated or change width across the well-developed axial planar foliations. For example, the coarse-grained, hornblende-rich melanocratic layer marked m1 in line drawing (lower part of image) is discontinuous across an axial planar foliation marked by hornblende grains spread along its length (Hbl on line drawing). Similarly, the mesocratic layer to the right of the coin changes width abruptly across the axial planar foliation. The leucosome layer in upper right is truncated by the axial planar foliation, on the other side of which there is instead a narrow melanosome (m3). Combined, these features suggest that layer-parallel leucosomes and melanosomes were extracted along the axial planar foliation, which are inferred to have acted as a melt conduit. All images from loose blocks.

Figure 7. Pegmatite accumulation on the concave side of a gently folded contact between metatexitic migmatite and amphibolite layer. Pegmatite intrudes amphibolite above and has diffuse contacts with migmatite below. Higher amplitude of pegmatite intrusion compared to that of the ghost stratigraphy in the migmatite-pegmatite transition zone (close to hammer) indicates pegmatite drainage from the migmatites. Loose block.

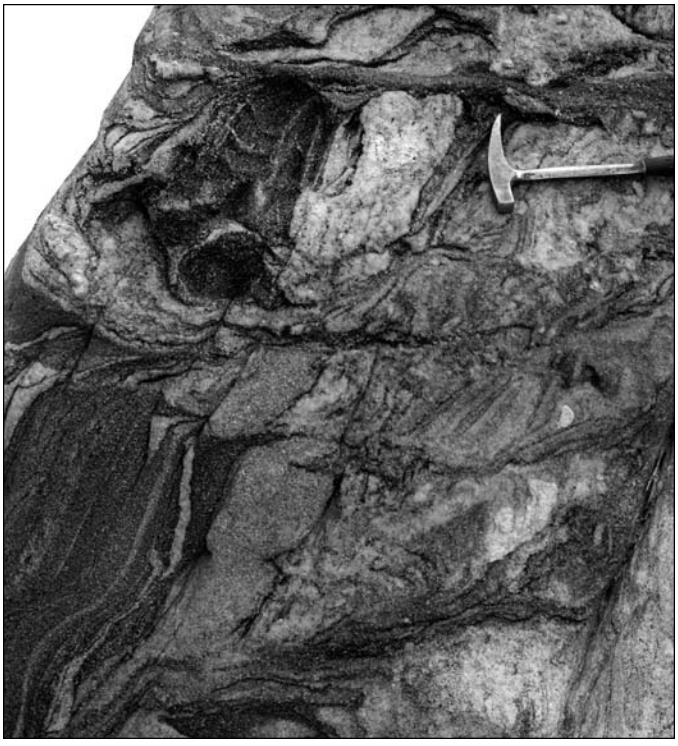

Figure 8. Leucosome cuts through, drags, and disaggregates layering. Schlieren cusps and increased disaggregation suggest leucosome flow to the right. Features are exaggerated by cut effect due to block surface being at 40° to migmatite layering.

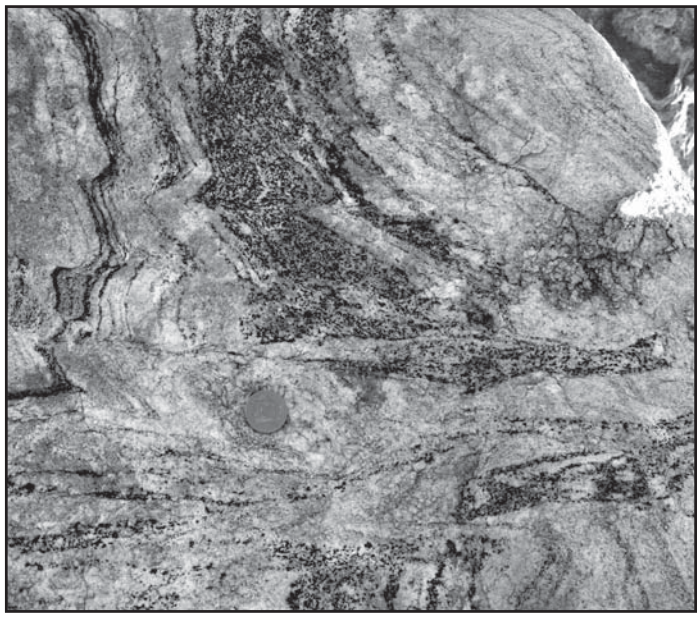

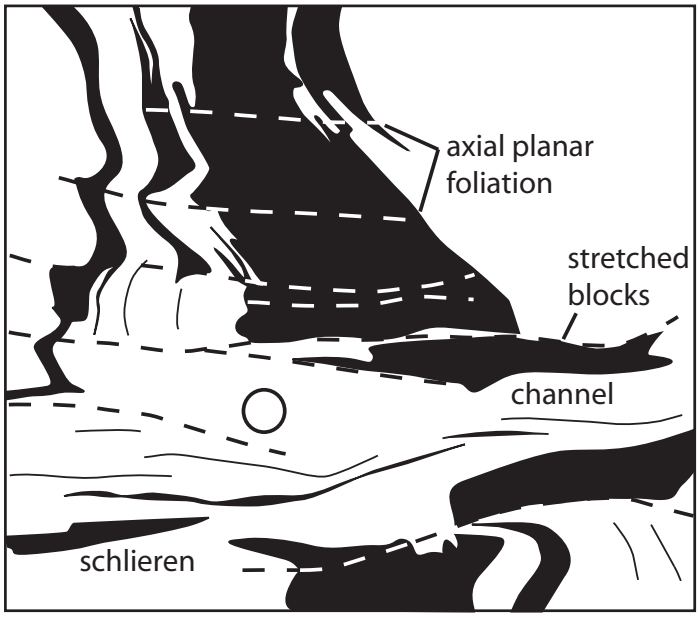

Figure 9. Gradual transposition of layers toward a hinge zone. Parasitic fold wavelength decreases and amplitude increases toward the transposed zone as a result of stretching and rotation of blocks. Ultimately, layers are truncated by the 10-cm-wide leucosome band with biotite-hornblende schlieren (lower central part of figure), interpreted to be a channel-way through which melt escaped, transposing layering caught up in the flow.

asymmetric folds is accompanied by layer rotation, disaggregation, and transposition.

Parasitic, asymmetric folds are separated by well-developed axial planar foliations defining asymmetric "parasitic fold blocks" (2 in Fig. 4A; Figs. 10 and 11). Typically the more external parasitic fold block, away from the hinge zone, is more stretched and rotated toward parallelism with the axial plane (Fig. 4B; 6 in Fig. 4A), which acts as a shear plane (Fig. 4B; 3 in Fig. 4A; Fig. 11A). Axial planar shear zones allow considerable relative movement between parasitic fold blocks (Fig. 12). Typically also, fold profiles within a parasitic fold block become gradually more rotated toward the transposition plane, until layering is transposed and the fold block is disrupted forming a diatexite (7 and vertical arrows labeled "rotation" in Fig. 4A). Parasitic fold blocks may also split or merge with other fold blocks giving rise to disharmonic folds (Fig. 11).

Leucosomes form a network where layer-parallel and axial planar leucosomes are linked continuously (e.g., Figs. 5 and 13). Individual axial planar leucosomes merge into and out of many layer-parallel leucosomes, suggesting it communicates with and transfers magma in and out of layer-parallel leucosomes. The interconnected system of leucosomes trends on average obliquely across the fold, at an angle to the axial planar foliation (Fig. 13) gradually migrating toward the fold closure and always broadly conformable with the shape of the fold. The oblique trend is achieved by axial-planar leucosomes side-stepping from the outer parts of fold limbs toward the hinge, using layer-parallel leucosomes (Fig. 13). Thus, if we view the leucosomes as representing magma pathways, magmas are not only segregated preferentially in fold hinge zones (Figs. 5B and 5C), but they also migrate diagonally across the fold toward the fold closure (Fig. 13). When reaching the hinge zone, diagonal migration stalls and leucosomes either truncate the opposite fold limb, or merge with other axial planar leucosomes (Fig. 4).

Axial planar leucosomes and zones where the main fabric has been transposed by folding commonly have blocks of melanocratic material, or irregular mafic schlieren. These are composed mainly of biotite and hornblende plus titanite, related to disaggregation of preexisting layering (Figs. 9 and 12B). Figure 12B shows significant reduction in the width of some melanocratic layers in the hinge of disharmonic folds. For example, layer m1 narrows abruptly from 14.5 cm to 0.5 cm in the fold in the center of the image, and layer m3 narrows continuously by a factor of 10 to form a narrow, melanocratic fold hinge. This pattern, suggests mobility not only of the leucocratic layers, but also of melanocratic layers, possibly related to magma flow erosion. This process could in part explain the melanocratic blocks and schlieren in axial planar leucosomes in Figures 6C and 13B.

The network of axial planar and layer-parallel leucosomes, the rotation of limbs, the shearing along axial planar foliations, the breakup of hinge zones, and layer disaggregation, all combined, lead to a complete disaggregation of the metatexite. The result is a diatexite characterized by numerous blocks of refractory material (e.g., Solar and Brown, 2001), mafic schlieren and fragments of early crystallized and disaggregated pegmatitic K-feldspar and biotite grains (Fig. 14A), and highly stretched asymmetric fold blocks (Fig. 14B).

DISCUSSION

Nature and Evolution of the Magma Network

The disharmonic folds typical of these metatexites suggest that the layered sequence behaved heterogeneously. This is likely a result of variations in melt distribution and rock strength, from grain to outcrop scale, combined with the ability of magma to migrate in response to local pressure variations during folding. The interconnected system of layer-parallel and axial planar leucosomes has been described also in a number of anatectic terranes (Brown, 1994; Collins and Sawyer, 1996; Hand and Dirks, 1992; McLellan, 1988; Sawyer et al., 1999; Vernon et al., 2003; Vernon and Paterson, 2001). In Tangtse, axial planar leucosomes have acted as magma removal pathways from within layers. This is evidenced by the dragging and disruption of fold hinges, as well as layer truncation (Figs. 6C and 12B). The general magma drainage was from pores into layer-parallel or axial planar leucosomes (Fig. 5), forming a network transporting magma diagonally across the fold from limbs to fold closures (Fig. 15). This pattern is likely repeated at all scales of folding, leading to communication and flow from the smallest parasitic fold to the largest fold closure in the system.

Metatexite breakup takes place at a number of scales and through a number of processes. At the decimeter to meter scale, layers rotate and stretch toward the axial planar orientation, magma in layer-parallel leucosomes are drained to form axial planar leucosomes (e.g., Fig. 6C), and in the process erode melanocratic layers that disaggregate to form schlieren (e.g., Fig. 6B). The evolution of an interconnected drainage network of melt-rich leucosomes undermines the solid framework of the metatexite, causing disaggregation and loss of continuity leading to fold breakup, with disruption of individual layers, or entire fold sections that become rafts in the diatexite (Fig. 14).

Evidence for magma ponding in fold hinges (Allibone and Norris, 1992; Sawyer et al., 1999) is relatively uncommon in the Tangtse diatexite. Generally, hinge zones have been disrupted and transposed by magmas, and ponding is only preserved in the vicinity of amphibolite layers, the most competent rock in the system. The cauliflower-shaped contact between pegmatite and amphibolite in Figure 7 suggests that the pegmatitic magma ponded underneath the amphibolite (Burg and Vanderhaeghe, 1993). We postulate that if magma in Figure 7 had been capable of breaking through the amphibolite layer, it would have drained from the underlying migmatite, leading to fold tightening and dragging of metatexite layers to form a cuspate fold hinge, forming features similar to those in Figure 6A. Thus, we suggest that magma ponding under amphibolite layers, such as in Figure 7, represents remnants of incipient folding stages, superseded everywhere else, where rocks were weaker and hinge zones were transposed.

Cuspate Folds and Magma Loss

The development of cuspate fold hinges can be divided into three stages: (a) during early fold stages, magma is mobilized along the axial plane (Fig. 5B) and ponds under competent layers (Fig. 7); (b) at some point magma breaks through fold hinges, dragging layers in the flow direction, causing cusps pointing in the direction of flow (Figs. 5C, 6A, and 6B); (c) magma withdrawal from the axial plane causes suturing of the fold hinge and leucosome-free cusps (Fig. 6C). During suturing, there may be a mismatch of layers on either side of axial plane, either as a result of shearing or rotation along the plane or differential volume loss from either side (Fig. 6C).

Cusps are the most obvious feature indicative of magma migration and mass loss. Evidence for mass loss can also be more subtle and take the form of variations in layer width or layer truncation across well-developed axial planar foliations. In Figure 6C, for example, leucosome and melanosome layers are truncated and discontinuous across such foliations (see also Fig. 6B). Evidence for mobilization of melanocratic layers is best depicted in Figure 12B by the narrowing of melanocratic layers. Although this could reflect primary width variations, the most likely explanation is that leucocratic magma eroded the melanocratic layers as it escaped into axial planar leucosomes, explaining the presence of irregular melanocratic blocks and mafic schlieren in the latter. Erosion of melanocratic layers would be favored where they have rela-

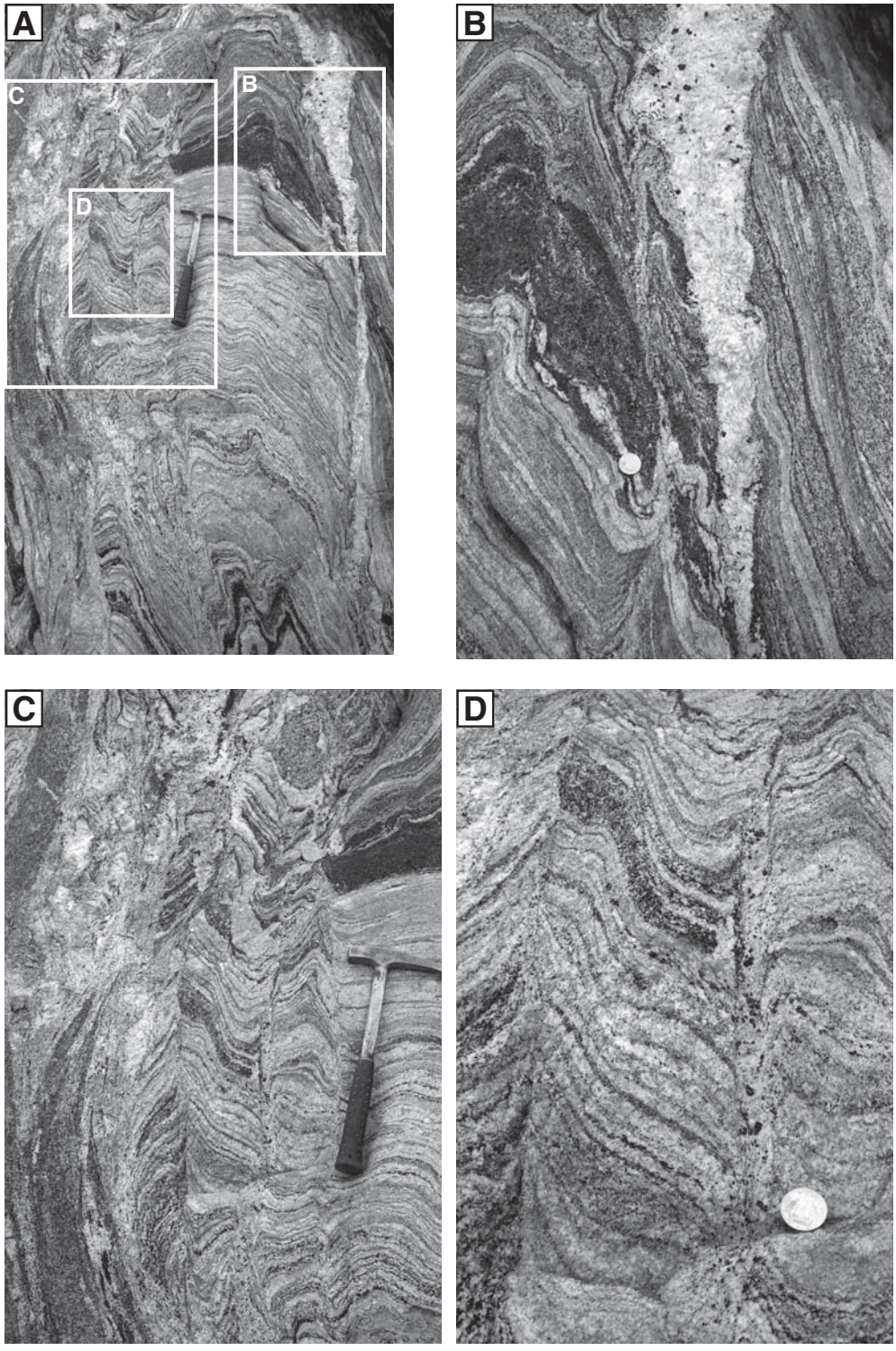

Figure 10. Overview and details of a steep exposure recording many features of the transposition process. (A) Metatexite fold preserved inside a generally transposed diatexite (left-hand side of image). Transposed layering strikes 120° and dips nearly vertically, and layering in metatexite is at high angle to transposition plane. (B) Detail of leucosome in the axial plane of a cuspate fold merging upward with a larger dike with euhedral porphyroblasts of hornblende (upper right-hand side). This dike is roughly parallel to the axial plane of the fold and widens upward. (C) Detail of transposed layering on left, and angular, cuspate folds on right, truncated along the hinge zone by axial planar foliation. Note truncation of the thick mafic layer above hammer by axial planar leucosome and fold train. Note also that these fold trains get disrupted and truncated by pegmatitic granite further up. Fold profiles just left of the hammer change from close angular in the upper part, to increasingly open downward (below hammer). (D) Detail of angular cuspate folds in (C) showing both layer truncation and continuity of layers across the axial planes with hornblende-bearing leucosome.

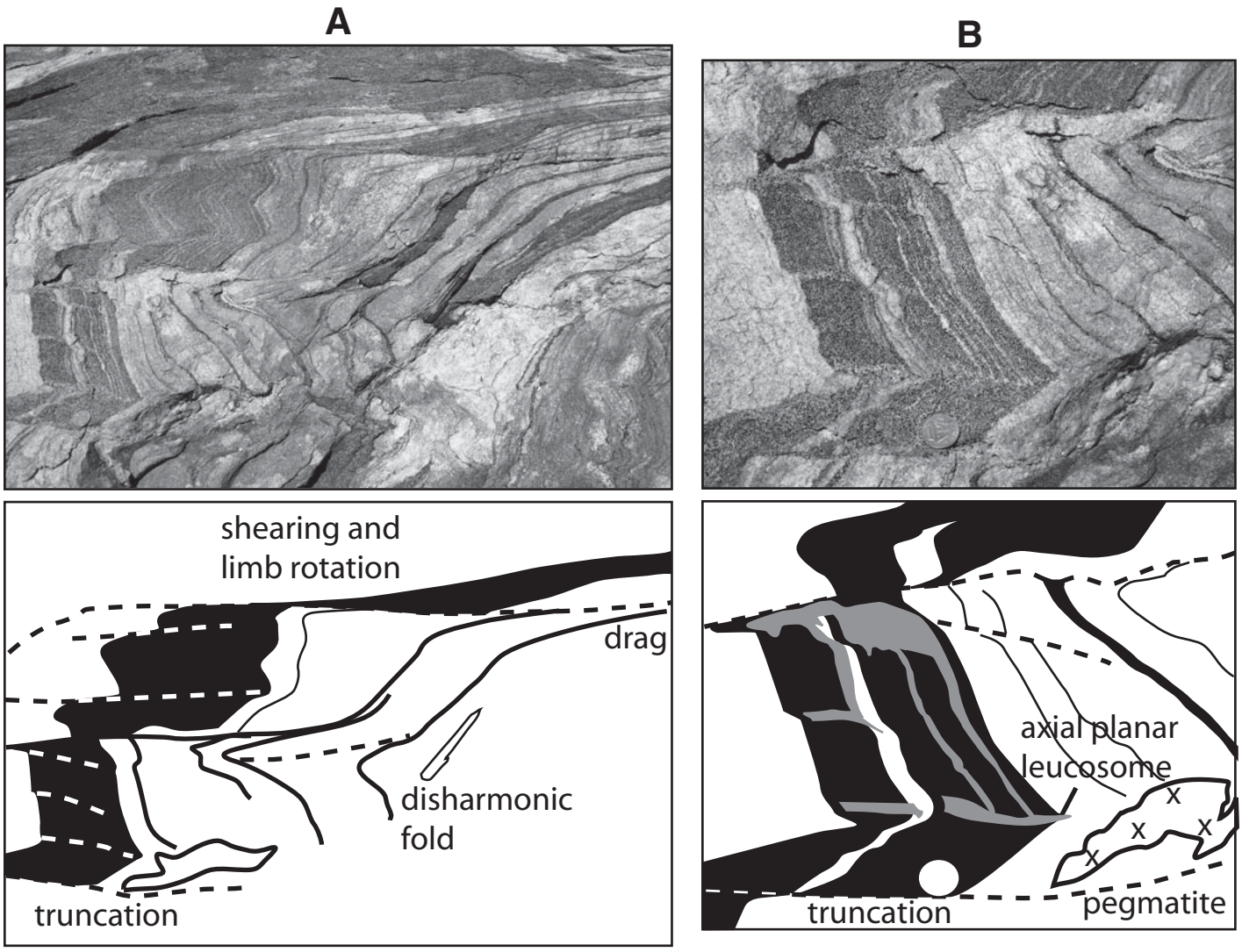

Figure 11. (A) Axial planar foliation in folded metatexite. Folds are disharmonic, and limb in the upper part of image is strongly stretched and rotated toward the axial planar orientation. Note pen close to the center as scale. (B) Detail of A, layers truncated by axial planar foliation, and angular fold with diffuse accumulation of leucocratic material along the hinge zone. Layers dip 50° into exposed surface.

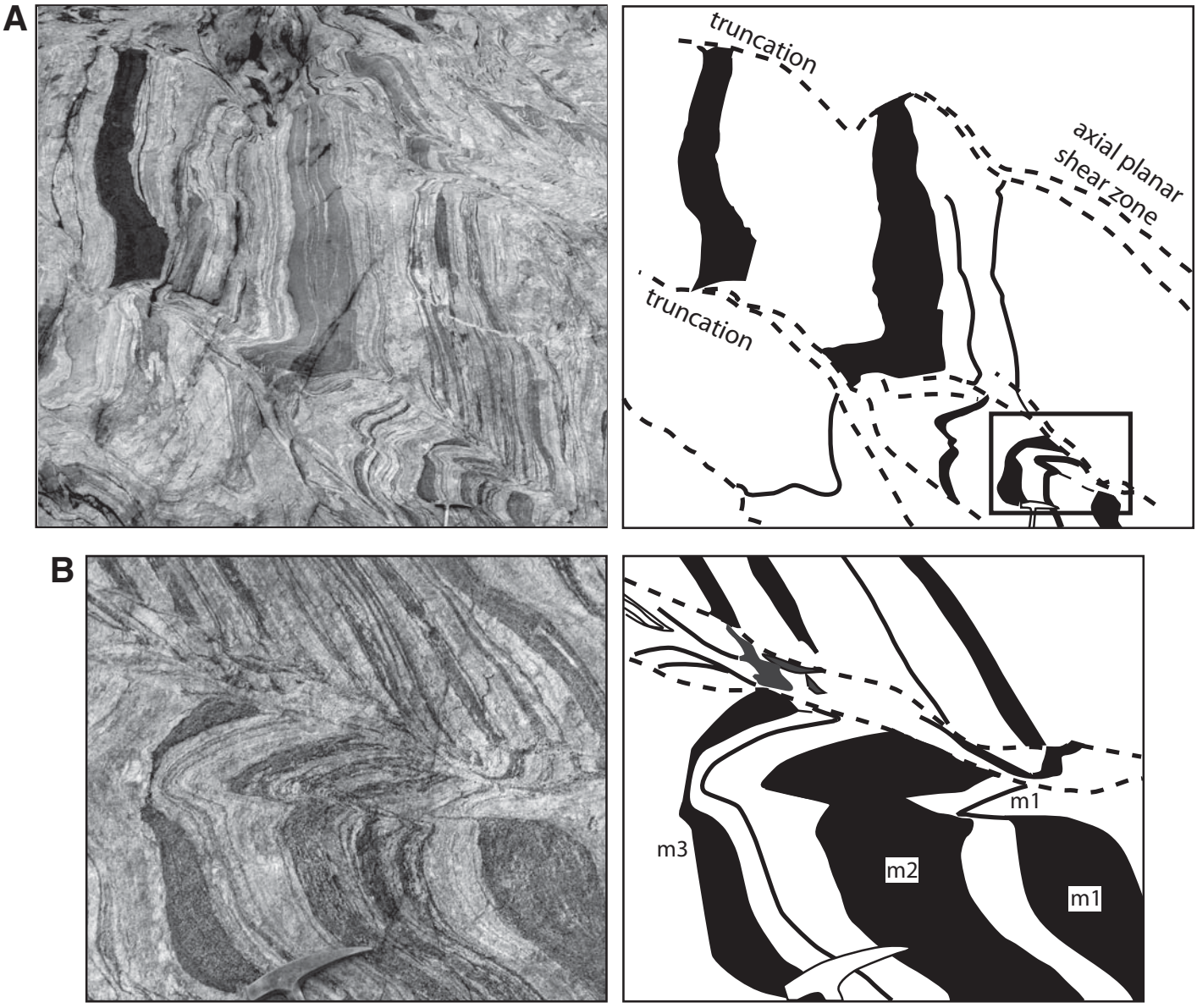

Figure 12. (A) Metatexite preserving primary banding at high angle to the axial plane of folds, which act as shear zones, truncating layering (e.g., amphibolite layer in upper left). Hammer for scale in lower right. Box shows the position of B. (B) Detail of disharmonic folds and layer truncation. Axial planar band contains partly disaggregated melanocratic bands and schlieren in granitic material. Layers in the upper half of the image are unrelated to those in the lower half. The melanocratic layer m1 thins to 1/30 of its width in the fold in the middle of the image, and layer m3 thins to 1/10 of its width in the hinge zone. These features suggest bulk mass loss, possibly recorded by disaggregated melanocratic material in axial planar transposed zones.

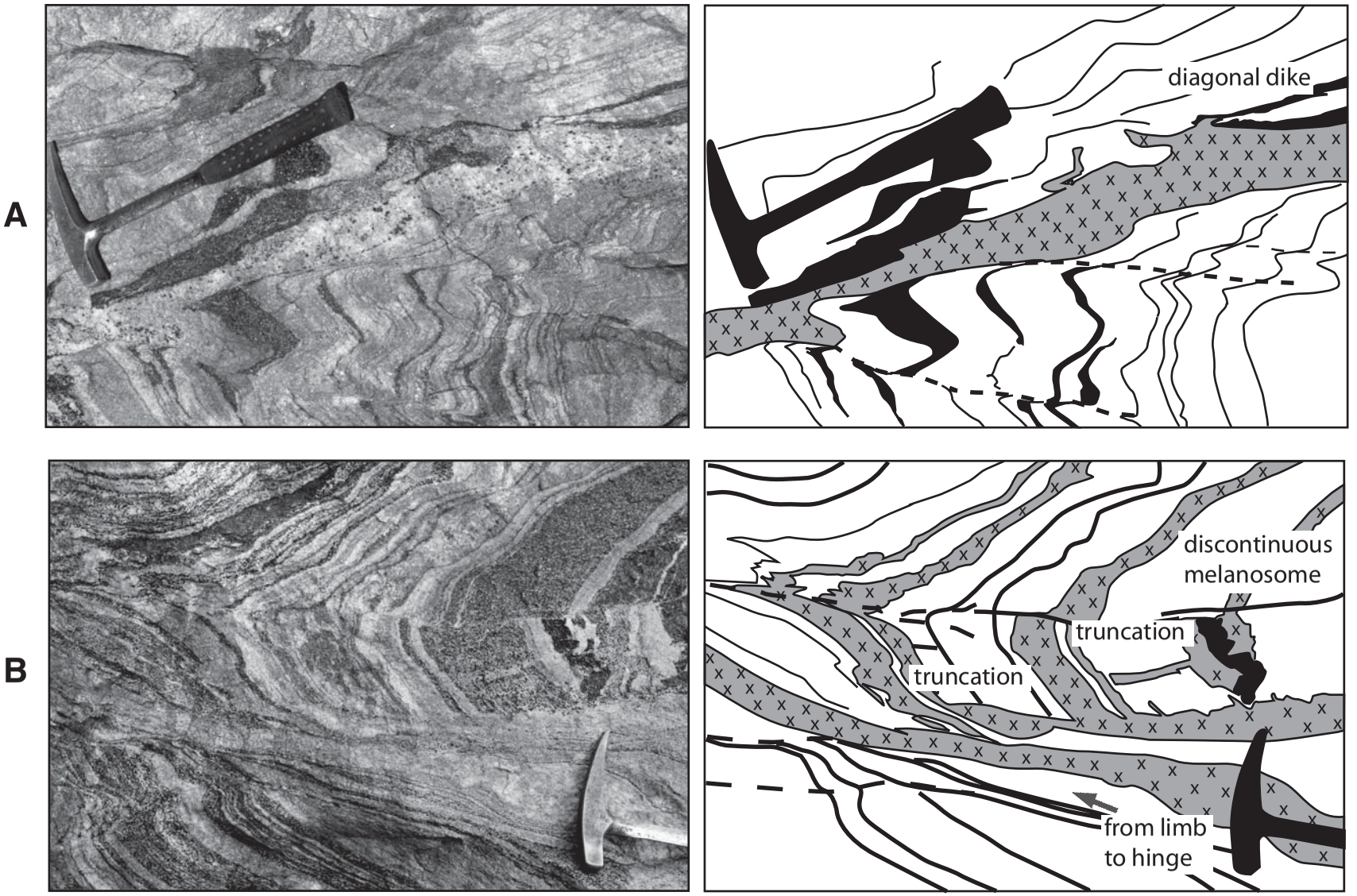

Figure 13. (A) Hornblende leucogranite traverses a fold limb alternating between conforming to folded layering and to the axial planar foliation, causing it to trend diagonally toward the hinge zone. (B) Axial planar leucosome (under hammer) truncating fold limb and stepping inward toward hinge zone. This leucosome is linked continuously with layer-parallel leucosomes (gray shading with crosses in line drawing). Fold profile changes from an open fold on the right into a sharp acute fold on the left. Layers on the lower limb (left of hammer) are strongly rotated toward the axial planar orientation. Note layer mismatch across the hinge line of the open fold and discontinuous melanosome (black in line drawing) in center-right of the image.

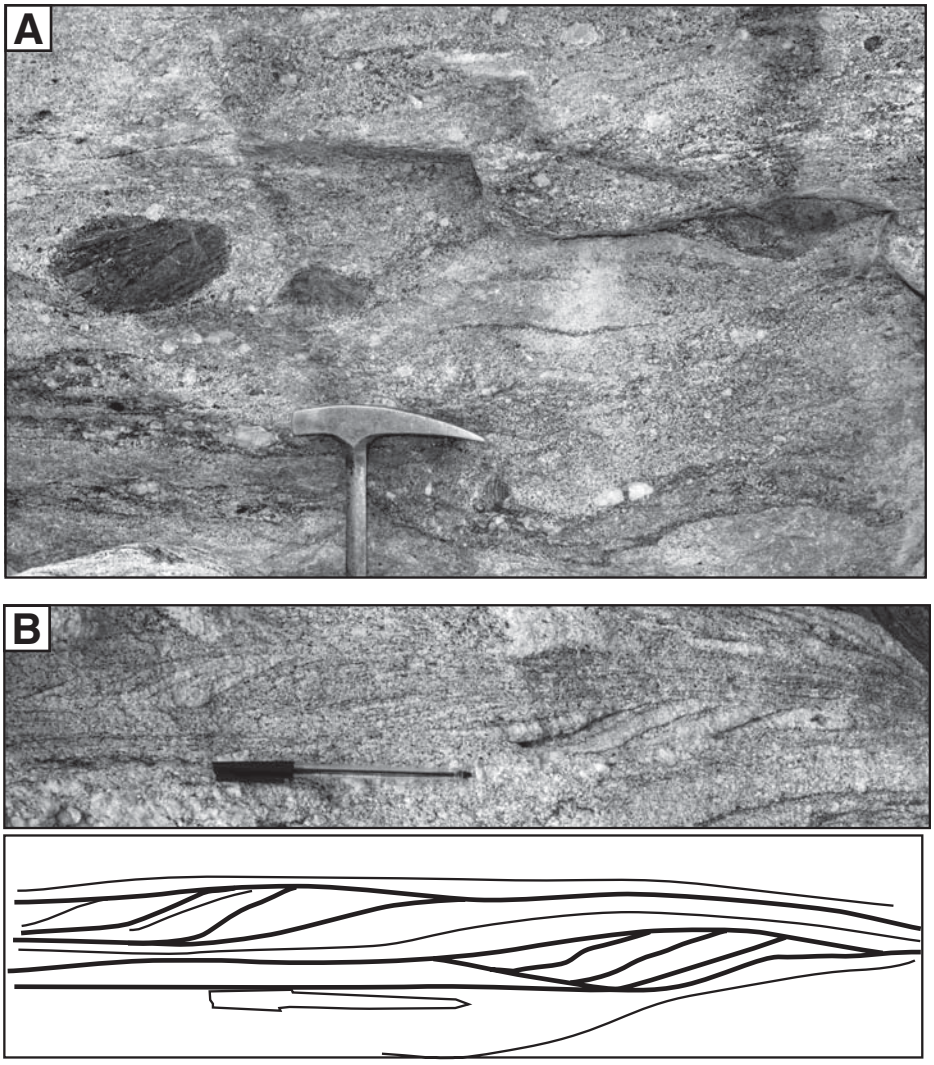

Figure 14. (A) Advanced stages of disaggregation forming a diatexite including numerous blocks and grains of refractory material, as well as schlieren and bands of different composition. (B) Diatexites preserve also parasitic fold trains recording late stages of transposition.

tively low viscosity due to the presence of melt, or where there was intense drag (a measure of magma velocity and viscosity) imparted by flowing magma.

Maximum Stretching Axis and Axial Planar Shearing

Fold transposition was achieved in part by stretching of fold limbs (Figs. 11 and 13B). Melt enhanced folding by allowing (a) slip along axial planar foliations, (b) significant limb stretching by slip along ductile, melt-rich layer-parallel leucosomes, and (c) by actively breaking through layering, particularly competent layers in fold hinges. Volume loss or volume redistribution related to magma flow could have played an equally important role but is less evident. Many melting experiments have demonstrated the importance of shear zones in melt extraction, generally oriented at the more characteristic acute angle to the maximum shortening direction instead of parallel to the fold axial plane (Rosenberg and Handy, 2001). The absence of these shear planes may be ascribed to relatively high-melt pore pressure that permitted activation of shear movement along axial plane surfaces, which have relatively small shear component on them. It is interesting to note that melting experiments have inferred that melt must have migrated along planes oriented at high angles to the shortening direction, as indicated by melt distribution after deformation (Dell'Angelo and Tullis, 1988; Rosenberg and Handy, 2001), despite the rarity of melt pockets in this orientation. The contrast to their conspicuous presence in the field may be related to differences in the nature and intensity of pressure gradients in experiments and nature.

We infer that the combination of magma flow, extraction, and axial planar shearing, has transferred mass within the folded rock so as to allow shortening perpendicular to the fold axial plane, and stretching perpendicular to the fold axis within the axial planar foliation (Fig. 15). This implies a maximum stretching axis, x, plunging 50° to 60° toward the SE. By contrast, the maximum stretching axis for the mylonitic zones of the Karakoram Shear Zone is inferred to plunge parallel to the stretching lineation in the mylonites, moderately to the NW. This 90° difference in stretching axes suggests strain partitioning during transpression into simple shear in mylonites, and pure shear in folds.

Axial Planar Leucosomes

Many migmatites worldwide are characterized by layer-parallel leucosomes linked continuously with leucosomes in shear planes—cutting, displacing, and dragging layering (e.g., Figs. 13–14 in Brown, 1994)—as expected from experiments. Many others, like the Tangtse migmatites, have axial planar leucosomes. What controls whether a leucosome set develops in shear zones or in axial planar orientation is an intriguing and important question because the answer underlies inferences regarding the orientation of stress axes during folding and magma migration (Vernon and Paterson, 2001). In Tangtse, magma drainage, combining axial planar and layer-parallel leucosomes, exploited the two most prominent weakness planes in the rock mass. This avoids the energy expenditure involved in creating new planes, such as cracks parallel to the maximum compressional stress axis or shear planes. More importantly, leucosome geometry establishes a wide magma network, with the two sets intersecting parallel to the fold axis (Fig. 15). This network weakens the rock mass, and accelerates mass transfer driven by pressure differences, increasing strain rates by accelerating fold amplification and transposition. Thus, contrary to a static perception of the system, axial planar magma-filled sheets in migmatites do not imply a bulk addition of mass in the direction of maximum shortening, as for dikes in brittle rocks. Rather, axial planar sheets represent the remnants of an efficient system that transferred mass through the deforming mass, accelerating shortening in the direction of maximum shortening axis and stretching in the direction of maximum stretching axis.

Therefore, it can be further inferred that axial planar leucosomes are only likely to develop in a system where they are capable of maximizing

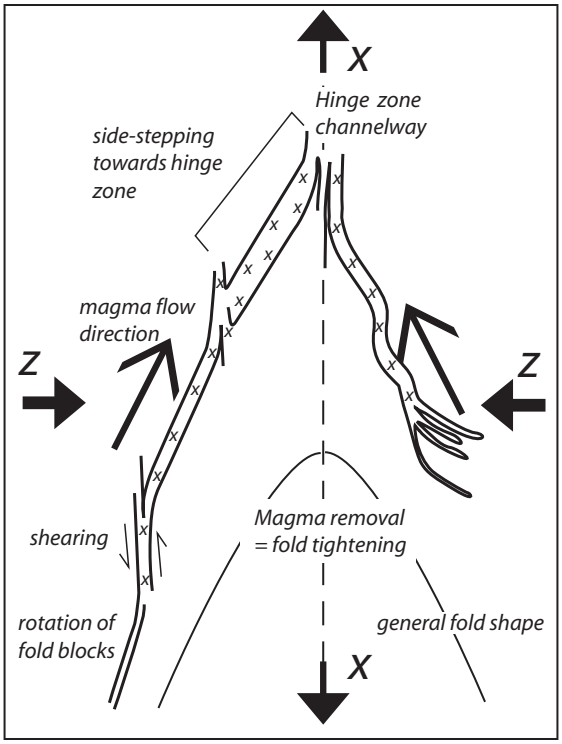

Figure 15. Sketch of the main features, strain axes, and magma migration direction inferred from field features linking folding and magma migration.

mass transfer and enhancing straining. If this mass transfer is inhibited at any scale, leucosomes might instead explore shear bands. Thus, the rise of a network including axial planar leucosomes is an energy efficient way of relaxing differential stresses. Vernon and Paterson (2001) suggested a number of valid reasons to account for axial planar leucosomes. The one proposed in this paper differs in that it takes into account their role in straining through maximizing mass transfer.

SENSE OF MAGMA MIGRATION

The most important indicators of the sense of magma migration in 2D fold profiles are: (a) the orientation of hinge cusps, (b) the accumulation of magma on only one side of a competent layer (Burg and Vanderhaeghe, 1993), and (c) the oblique migration of leucosomes from fold limbs to closures, broadly concordant with the general shape of the fold (Fig. 15). These features suggest a flow component perpendicular to the fold axis, parallel to the inferred maximum stretching axis. Evidence for both upward and downward magma flow parallel to the stretching axis was found in the same outcrop or block. However, some outcrops presented asymmetries suggestive of preferential upward magma migration. We documented a number of times the presence of well-developed antiformal fold closures, sometimes side-by-side, without intervening synformal closures (Fig. 3). This suggests that synforms may have been preferentially stretched and transposed (similar to outcrops in central Australia; Sawyer et al., 1999). Unfortunately, we do not have statistically meaningful determination of preferential sense of magma flow.

Folds, because of their geometry, have markers that record magma flow perpendicular to the fold axis, along the axial planar foliation. However, folds lack indicators to record magma migration parallel to the fold axis. This imposes a natural bias to the observations so that the question of whether there was significant magma flow parallel to the fold axis cannot be easily answered. Despite this bias, the lack of an obvious mechanism to impose a pressure gradient to drive magma flow parallel to the fold axis, suggests that only a minor component of magma migration would have taken place in this direction (see also Brown and Solar, 1998).

CONCLUSIONS

Delicate structures preserved in the migmatites at Tangtse reveal details of the interplay between magma migration and folding (Fig. 15). The two processes act in tandem and reinforce each other. Folding gives rise to the pressure gradients that drive magma migration and give rise to the network of layer-parallel and axial planar sheets, now preserved as leucosomes, that drains and disrupts the metatexite to produce the diatexite. Magma migration, in turn, arguably increases the rate of folding by efficiently transferring material to low-pressure sites. Folding and rock disaggregation develop as a result of this organized network of leucosomes. Features such as cuspate hinges, side-stepping of axial planar leucosomes toward the hinge zone, the abrupt truncation of layers by axial planar shear zones, the removal of leucosomes and the dragging of melanosomes to form mafic schlieren or mafic blocks, and disharmonic folds, are all part of a single system that maximizes mass transfer and stress release. The question regarding the formation of leucosomes in the seemingly unfavorable axial planar orientation, at high angle to the statistical orientation of the maximum shortening axis, is resolved by considering it in this dynamic context. These leucosomes are remnants of magma escape pathways that allowed faster shortening parallel to the maximum shortening axis, and thus effectively relaxed differential stresses. Thus, it is this increased rate of strain by volume loss that stabilizes the development of axial planar leucosomes.

ACKNOWLEDGMENTS

We thank Henning Reichardt for discussions in the field and Andy Tomkins and Claudio Rosenberg for constructive reading of an early version of the manuscript. We thank also Mike Brown, Bob Miller, and Calvin Miller for their constructive and detailed reviews.

REFERENCES CITED

Allibone, A.H., and Norris, R.J., 1992, Segregation of leucogranite microplutons during syn-anatectic deformation: An example from the Taylor Valley, Antarctica: Journal of Metamorphic Geology, v. 10, p. 589–600, doi: 10.1111/j.1525-1314.1992.tb00107.x.

Berger, A., Burri, T., Alt-Epping, P., and Engi, M., 2007, Tectonically controlled fluid flow and water-assisted melting in the middle crust: An example from the Central Alps: Lithos, 18 p., doi: 10.1016/j.lithos.2007.07.027, in press.

Brown, E.T., Bendick, R., Bourles, D.L., Gaur, V., Molnar, P., Raisbeck, G.M., and Yiou, F., 2002, Slip rates of the Karakorum fault, Ladakh, India, determined using cosmic ray exposure dating of debris flows and moraines: Journal of Geophysical Research, v. 107, article no. 2192.

Brown, M., 1973, The definition of metatexis, diatexis and migmatite: Proceedings of the Geologists' Association, v. 84, no. 4, p. 371–382.

Brown, M., 1978, The tectonic evolution of the Precambrian rocks of the St. Malo region, Armorican Massif, France: Precambrian Research, v. 6, p. 1–21, doi: 10.1016/0301-9268(78)90052-9.

Brown, M., 1994, The generation, segregation, ascent and emplacement of granite magma: The migmatite-to-crustally derived granite connection in thickened orogens: Earth-Science Reviews, v. 36, p. 83–130, doi: 10.1016/0012-8252(94)90009-4.

Brown, M., 2005, The mechanisms of melt extraction from lower continental crust of orogens: Is it a self-organized critical phenomenon?: Transactions of the Royal Society of Edinburgh: Earth Sciences, v. 95, p. 35–48.

Brown, M., and D'Lemos, R.S., 1991, The Cadomian granites of Mancellia, north-east Armorican Massif of France: Relationship to the St. Malo migmatite belt, petrogenesis and tectonic setting: Precambrian Research, v. 51, p. 393–427, doi: 10.1016/0301-9268(91)90110-V.

Brown, M., and Solar, G.S., 1998, Shear-zone systems and melts: Feedback relations and self-organization in orogenic belts: Journal of Structural Geology, v. 20, no. 2–3, p. 211–227, doi: 10.1016/S0191-8141(97)00068-0.

Burg, J.-P., and Vanderhaeghe, O., 1993, Structures and way-up criteria in migmatites, with applications to the Velay dome (French Massif Central): Journal of Structural Geology, v. 15, no. 11, p. 1293–1301, doi: 10.1016/0191-8141(93)90103-H.

Collins, W.J., and Sawyer, E.W., 1996, Pervasive granitoid magma transfer through the lower-middle crust during non-coaxial compressional deformation: Journal of Metamorphic Geology, v. 14, p. 565–579, doi: 10.1046/j.1525-1314.1996.00442.x.

Dell'Angelo, L.N., and Tullis, J., 1988, Experimental deformation of partially melted granitic aggregates: Journal of Metamorphic Geology, v. 6, p. 495–515, doi: 10.1111/j.1525-1314.1988.tb00436.x.

D'Lemos, R.S., Brown, M., and Strachan, R.A., 1992, Granite magma generation, ascent and emplacement within a transpressional orogen: London, Journal of the Geological Society, v. 149, p. 487–490.

Dunlap, W.J., Weinberg, R.F., and Searle, M.P., 1998, Karakoram fault zone rock cool in two phases: London, Journal of the Geological Society, v. 155, p. 903–912.

Greenfield, J.E., Clarke, G.L., and White, R.W., 1998, A sequence of partial melting reactions at Mt. Stafford, central Australia: Journal of Metamorphic Geology, v. 16, p. 363–378, doi: 10.1111/j.1525-1314.1998.00141.x.

Hand, M., and Dirks, P.H.G.M., 1992, The influence of deformation on the formation of axial-planar leucosomes and the segregation of small melt bodies within the migmatitic Napperby Gneiss, central Australia: Journal of Structural Geology, v. 14, no. 5, p. 591–604, doi: 10.1016/0191-8141(92)90159-T.

Hollister, L.S., and Crawford, M.L., 1986, Melt-enhanced deformation: A major tectonic process: Geology, v. 14, p. 558–561, doi: 10.1130/0091-7613(1986)14<558:MDAMTP>2.0.CO;2.

Honegger, K., Dietrich, V., Frank, W., Gansser, A., Thöni, M., and Trommsdorff, V., 1982, Magmatism and metamorphism in the Ladakh Himalayas (the Indus-Tsangpo suture zone): Earth and Planetary Science Letters, v. 60, p. 253–292, doi: 10.1016/0012-821X(82)90007-3.

Hutton, D.H.W., and Reavy, R.J., 1992, Strike-slip tectonics and granite petrogenesis: Tectonics, v. 11, no. 5, p. 960–967.

Lappin, A.R., and Hollister, L.S., 1980, Partial melting in the Central Gneiss Complex near Prince Rupert, British Columbia: American Journal of Science, v. 280, p. 518–545.

Marchildon, N., and Brown, M., 2003, Distribution of melt-bearing structures in anatectic rocks from Southern Brittany, France: Implications for melt transfer at grain- to orogen-scale: Tectonophysics, v. 364, p. 215–235, doi: 10.1016/S0040-1951(03)00061-1.

McLellan, E.L., 1988, Migmatite structures in the Central Gneiss Complex, Boca de Quadra, Alaska: Journal of Metamorphic Geology, v. 6, p. 517–542, doi: 10.1111/j.1525-1314.1988.tb00437.x.

Miller, C.F., Watson, M.E., and Harrison, T.M., 1988, Perspective on the source, segregation and transport of granitoid magmas: Transactions of the Royal Society of Edinburgh: Earth Sciences, v. 79, p. 135–156.

Milord, I., Sawyer, E.W., and Brown, M., 2001, Formation of diatexite migmatite and granite magma during anatexis of semi-pelitic metasedimentary rocks: An example from St. Malo, France: Journal of Petrology, v. 42, no. 3, p. 487–505, doi: 10.1093/petrology/42.3.487.

Mogk, D.W., 1992, Ductile shearing and migmatization at mid-crustal levels in an Archaean high-grade gneiss belt, northern Gallatin Range, Montana, USA: Journal of Metamorphic Geology, v. 10, p. 427–438, doi: 10.1111/j.1525-1314.1992.tb00094.x.

Molnar, P., and Tapponnier, P., 1975, Cenozoic tectonics of Asia: Effects of a continental collision: Science, v. 189, p. 419–426, doi: 10.1126/science.189.4201.419.

Molnar, P., and Tapponnier, P., 1978, Active tectonics of Tibet: Journal of Geophysical Research, v. 83, p. 5361–5375.

Phillips, R.J., Parrish, R.R., and Searle, M.P., 2004, Age constraints on ductile deformation and long-term slip rates along the Karakoram fault zone, Ladakh: Earth and Planetary Science Letters, v. 226, p. 305–319, doi: 10.1016/j.epsl.2004.07.037.

Ravikant, V., 2006, Utility of Rb-Sr geochronology in constraining Miocene and Cretaceous events in the eastern Karakoram, Ladakh, India: Journal of Asian Earth Sciences, v. 27, p. 534–543.

Rolland, Y., and Pêcher, A., 2001, The Pangong granulites of the Karakoram Fault (Western Tibet): Vertical extrusion within a lithosphere-scale fault?: Comptes Rendus de L'Académie des Sciences, Serie II: Sciences de la Terre et des Planètes, v. 332, p. 363–370.

Rosenberg, C.L., and Handy, M.R., 2001, Mechanisms and orientation of melt segregation paths during pure shearing of a partially molten rock analogue (norcamphor-benzamide): Journal of Structural Geology, v. 23, p. 1917–1932, doi: 10.1016/S0191-8141(01)00037-2.

Rosenberg, C.L., and Handy, M.R., 2005, Experimental deformation of partially melted granite revisited: Implications for the continental crust: Journal of Metamorphic Geology, v. 23, p. 19–28, doi: 10.1111/j.1525-1314.2005.00555.x.

Sawyer, E.W., 1991, Disequilibrium melting and the rate of melt-residuum separation during migmatization of mafic rocks from the Grenville Front, Quebec: Journal of Petrology, v. 32, p. 701–738.

Sawyer, E.W., 1998, Formation and evolution of granite magmas during crustal reworking: the significance of diatexites: Journal of Petrology, v. 39, no. 6, p. 1147–1167, doi: 10.1093/petrology/39.6.1147.

Sawyer, E.W., 1999, Criteria for the recognition of partial melting: Physical and Chemistry of the Earth (A), v. 24, no. 3, p. 269–279, doi: 10.1016/S1464-1895(99)00029-0.

Sawyer, E.W., Dombrowski, C., and Collins, W.J., 1999, Movement of melt during synchronous regional deformation and granulite-facies anatexis: An example from the Wuluma Hills, central Australia, *in* Castro, A., Fernandez, C., and Vigneresse, J.L., eds., Understanding granites: Integrating new and classical techniques: London, Geological Society of London, Special Publications, p. 221–237.

Searle, M.P., Weinberg, R.F., and Dunlap, W.J., 1998, Transpressional tectonics along the Karakoram Fault Zone, northern Ladakh, *in* Holdsworth, R.E., and Strachan, R.A., eds., Continental transpressional and transtensional tectonics: London, Geological Society of London, Special Publications, p. 307–326.

Solar, G.S., and Brown, M., 2001, Petrogenesis of migmatites in Maine, USA: Possible source of peraluminous leucogranite in plutons?: Journal of Petrology, v. 42, p. 789–823, doi: 10.1093/petrology/42.4.789.

Spear, F.S., 1993, Metamorphic phase equilibria and pressure-temperature-time paths: Mineralogical Society of America, 799 p.

Valli, F., Nicolas, A., Leloup, P.H., Sobel, E.R., Mahéo, G., Lacassin, R., Guillot, S., Li, H., Tapponnier, P., and Xu, Z., 2007, Twenty million years of continuous deformation along the Karakorum fault, western Tibet: A thermochronological analysis: Tectonics, v. 26, doi: 10.1029/2005TC001913, doi: 10.1029/2005TC001913.

van der Molen, I., and Paterson, M.S., 1979, Experimental deformation of partially melted granite: Contributions to Mineralogy and Petrology, v. 70, p. 299–318, doi: 10.1007/BF00375359.

Vernon, R.H., and Paterson, S.R., 2001, Axial-surface leucosomes in anatectic migmatites: Tectonophysics, v. 335, p. 183–192, doi: 10.1016/S0040-1951(01)00049-X.

Vernon, R.H., Collins, W.J., and Richards, S.W., 2003, Contrasting magmas in metapelitic and metapsammitic migmatites in the Cooma Complex, Australia: Visual Geosciences, doi: 10.1007/s10069-003-0010-1.

Vigneresse, J.L., Barbey, P., and Cuney, M., 1996, Rheological transitions during partial melting and crystallization with application to felsic magma segregation and transfer: Journal of Petrology, v. 37, no. 6, p. 1579–1600, doi: 10.1093/petrology/37.6.1579.

Weinberg, R.F., 1999, Mesoscale pervasive melt migration: alternative to dyking: Lithos, v. 46, no. 3, p. 393–410, doi: 10.1016/S0024-4937(98)00075-9.

Weinberg, R.F., and Dunlap, W.J., 2000, Growth and deformation of the Ladakh Batholith, Northwest Himalayas: Implications for timing of continental collision and origin of calc-alkaline batholiths: The Journal of Geology, v. 108, p. 303–320, doi: 10.1086/314405.

Weinberg, R.F., and Searle, M.P., 1998, The Pangong Injection Complex, Indian Karakoram: A case of pervasive granite flow through hot viscous crust: London, Journal of the Geological Society, v. 155, p. 883–891.

Weinberg, R.F., Dunlap, W.J., and Whitehouse, M., 2000, New field, structural and geochronological data from the Shyok and Nubra valleys, northern Ladakh: Linking Kohistan to Tibet, *in* Khan, A., Treloar, P.J., and Searle, M.P., eds., Tectonics of the Nanga Parbat syntaxis and the Western Himalaya: London, Geological Society of London, Special Publications, p. 253–275.

White, R.W., Pomroy, N.E., and Powell, R., 2005, An in situ metatexite-diatexite transition in upper amphibolite facies rocks from Broken Hill, Australia: Journal of Metamorphic Geology, v. 23, p. 579–602, doi: 10.1111/j.1525-1314.2005.00597.x.

Manuscript received 15 March 2007
Revised manuscript received 20 August 2007
Manuscript accepted 9 October 2007

Printed in the USA